SRYAHWA PUBLICATIONS

Journal of Biotechnology and Bioengineering
ISSN: 2637-5362 | Volume 8, Issue 2, 2025
https://doi.org/10.22259/2637-5362.0802001

RESEARCH ARTICLE

Engineering Protein-Anthocyanin Complexes from Purple Sweet Potato (*Dioscorea alata*): Structural, Physicochemical, and Functional Characterization

Huy Loc Nguyen, Mauricio Martinon Gaspar

Department of Biological and Agricultural Engineering, Texas A&M University, College Station, TX 77843-2117, USA.

Received: 25 November 2025 Accepted: 10 December 2025 Published: 15 December 2025

Corresponding Author: Huy Loc Nguyen, Department of Biological and Agricultural Engineering,Texas A&M University, College Station, USA.

Abstract

This study investigated the ability of three protein matrices, including α-lactalbumin (α-L), whey protein isolate (WPI), and soy protein isolate (SPI), to encapsulate and stabilize anthocyanins (ACNs) isolated from purple sweet potato (PSP) through electrostatic precipitation, emphasizing their effects on entrapment efficiency, viscoelastic behavior, and particle morphology. PSP-ACNs were extracted, standardized as cyanidin-3-glucoside equivalents, and incorporated into protein solutions at concentrations ranging from 2 to 25 mg/L. Entrapment efficiency (EE%) and ACN-to-protein ratios increased significantly ($p < 0.05$) with rising anthocyanin concentrations for all proteins, with α-L consistently achieving the highest EE (up to 97.29%) due to its flexible conformation and abundance of reactive amino acid residues. WPI demonstrated similar performance at higher concentrations, whereas SPI exhibited lower EE at low ACN levels but approached comparable encapsulation efficiency near saturation. Rheological analyses revealed contrasting microstructural behaviors: α-L and WPI formed weak, dynamic viscoelastic fluids with G′–G″ crossover points, while SPI generated strong, elastic networks (G′ > G″) across all concentrations. Increasing ACN concentration caused reductions in storage and loss moduli and lowered critical frequency values, indicating weakened structural integrity under oscillatory stress. Transmission electron microscopy showed predominantly spherical nanoparticles (12–45 nm), with α-L exhibiting the most uniform and densely packed ACN distribution, WPI forming slightly larger aggregates, and SPI displaying irregular ellipsoids under high ACN loading. Collectively, these results demonstrate that protein type and ACN concentration govern molecular interactions, mechanical stability, and encapsulation behavior within PSP-ACN complexes, highlighting α-L and WPI as promising carriers for stabilizing anthocyanins in functional foods and nutraceutical formulations, while SPI offers potential for plant-based systems when properly optimized.

Keywords: Anthocyanins, α-Lactalbumin, Soy Protein, Whey Protein, Isolate.

1. Introduction

Food products should not only provide a significant dose of bioactive molecules but also ensure that these molecules remain fully functional, stable, and biologically accessible for as long as necessary during processing, storage, and digestion (Jacquier et al., 2024). Polyphenols, a diverse class of highly bioactive plant metabolites, constitute a critical part of the human diet, and extensive epidemiological and biochemical evidence supports their role in mitigating oxidative stress, inflammation, and chronic conditions such as cancer and cardiovascular diseases. Flavonoids represent approximately two-thirds of total dietary polyphenol intake, while derivatives of phenolic acids, particularly anthocyanins, account for the remaining one-third (Han et al., 2007). Their functional significance lies not only in their potent antioxidant capacity but also in their ability to modulate cellular signaling pathways related to metabolic and immune functions.

Anthocyanins (ACN) are a major subclass of water-soluble flavonoid pigments responsible for the vivid red, purple, and blue hues found in numerous fruits, vegetables, and flowers (He & Giusti, 2010; Oidtmann et al., 2012; Pojer, Johnson & Stockley, 2013). Beyond their colorant properties, these compounds

Citation: Huy Loc Nguyen, Mauricio Martinon Gaspar. Engineering Protein-Anthocyanin Complexes from Purple Sweet Potato (*Dioscorea alata*): Structural, Physicochemical, and Functional Characterization. Journal of Biotechnology and Bioengineering. 2025; 8(2): 1-12.

have been widely recognized for their antioxidant, anti-inflammatory, and anti-carcinogenic effects, which have spurred their incorporation into functional and nutraceutical food formulations. In particular, the development of value-added health foods utilizing purple sweet potato (PSP) has gained popularity due to its exceptionally high anthocyanin content, ranging from 84 to 174 mg per 100 g, far surpassing that of many other plant sources (Bovell-Benjamin, 2007; Suda et al., 2008; Bridgers, Chin & Vanden, 2010; Ray, Panda, Swain & Sivakumar, 2012). The dominant anthocyanin components in PSP are cyanidin acylglucosides and peonidin acylglucosides, which possess acylated structures contributing to enhanced pigment stability (Sun, Lu, Hao, Wu, Zhao & Wang, 2015).

Although acylated anthocyanins from PSP can be absorbed in their intact forms by rats and humans, their overall stability and bioactivity are highly susceptible to physicochemical degradation in both in vivo and in vitro conditions (Suda et al., 2002). Numerous intrinsic and extrinsic factors, including molecular structure, pH, temperature, light exposure, oxygen, metal ions, and interactions with coexisting compounds such as copigments, sugars, proteins, and degradation products, can profoundly influence their color intensity and chemical stability (Ma, 2004; Lu et al., 2015; Ma et al., 2016). Compounding these challenges, the gastrointestinal absorption of anthocyanins is relatively inefficient, often less than 5% for certain derivatives, thereby limiting their systemic bioavailability and diminishing their potential health-promoting effects (Ichiyanagi, 2008).

Conventional encapsulation strategies for polar bioactive compounds, such as liposomal entrapment or carbohydrate-based microencapsulation, have shown limited success in preserving anthocyanin integrity throughout digestion. These approaches frequently inadequately safeguard the molecules from enzymatic and pH-induced breakdown, resulting in the generation of structurally modified metabolites with reduced activity. Consequently, there is an urgent requirement for sophisticated molecular assemblies or tailored carrier systems that can protect flavonoids along the gastrointestinal tract while improving their stability, retention, and absorption (Woodward, Kroon, Cassidy & Kay, 2009; Kamonpatana et al., 2012; Liu et al., 2014, Liu et al., 2015; Lu et al., 2015).

In this context, structurally designed protein-based matrices have emerged as promising carriers for the targeted delivery of polyphenols. These matrices not only improve the physicochemical stability of the encapsulated compounds but also facilitate their release at specific sites within the body. Polyphenols in natural foods frequently form conjugates with proteins, generating soluble or insoluble complexes that exhibit enhanced resistance to oxidative or enzymatic degradation (Parada & Aguilera, 2007; Crowe, 2013). Accordingly, protein-rich ingredients, such as casein, whey, and plant-derived proteins, are being extensively explored for their binding affinity with anthocyanins, which enhances pigment stability and retention in functional foods (Gunasekaran, Ko, & Xiao, 2007; Ribnicky et al., 2014).

Among the encapsulation techniques that rely on protein aggregation, electrostatic precipitation stands out as a unique and reversible process that preserves the native structure of the protein (Puerta-Gomez & Castell-Perez, 2016). This approach offers multiple advantages, including low cost, minimal equipment requirements, operational simplicity, and the ability to perform at ambient or low temperatures, conditions particularly favorable for thermolabile compounds like anthocyanins. The resulting aggregates tend to remain stable during long-term storage and exhibit superior encapsulation efficiency compared to conventional industrial techniques such as spray drying in carbohydrate matrices (Harrison, Todd, Rudge & Petrides, 2003). Consequently, electrostatic precipitation represents a viable, scalable, and sustainable approach for entrapment and protection of anthocyanins, thereby enhancing their functional delivery and overall bioavailability.

The primary goal of this study was accomplished by addressing two specific objectives:

- Investigate the physicochemical impact of protein matrices sourced from plant and animal origins on the formation, size, and stability of anthocyanins (Cyanidin-3-Glucoside (C3G)) extracted from Purple Sweet Potato (Dioscorea alata).
- Characterize the functional and other performance properties of the protein-based complexes in terms of entrapment efficiency, morphology, and stability, by examining the interactions within the protein-anthocyanin interface via rheological analysis.

2. Materials and Methods

2.1 Anthocyanin (ACN) Isolation

Purple sweet potato extract (Dioscorea alata) was obtained from Avoca Inc. (Merry Hill, NC), and anthocyanin (ACN) was isolated by partitioning from a 10g reversed-phase Sep-Pak C18 20 cc cartridge (Waters Corporation, Milford, MA) that was previously conditioned with methanol and rinsed with deionized water to remove any polar constituents. Next, ethyl acetate was added to elute

the majority of phenolic acids and flavonoids, and PSP-ACN was recovered with acidified methanol (0.01% HCl), concentrated following solvent evaporation under vacuum at 30°C, and stored at 4°C until further analysis (Pacheco-Palencia, & Talcott, 2007).

Concentrated PSP-ACNs were standardized to a stock concentration in terms of mg of Cyanidin-3-Glucoside (C3G) equivalents/L using the Wrolstad's pH differential method of Wrolstad (2002). The anthocyanin monomeric pigment concentration (MAC) in the original samples was obtained using Eq. (1) and assuming a path length of 1 cm:

$$MAC\ (mg/L) = (A\ x\ Mw\ x\ D_F\ x\ 1000)/\ (\varepsilon\ x\ l) \quad (1)$$

where Mw is the molecular weight, D_F is the dilution factor, and is the molar absorptivity.

Cyanindin 3-glucoside (C3G) is used as the reference pigment with a = 449.2 g/mol and = 26,900 (10^6 L/mol cm). The absorbance of the diluted sample (A) was calculated as:

$$A = (A_{\lambda vis-max} - A_{700})_{pH=1.0} - (A_{\lambda vis-max} - A_{700})_{pH=4.5} \quad (2)$$

2.2 Sample Preparation

Four different concentrations of PSP- ACN stock solution (2, 5, 15, and 25 mg) were mixed with 20 µM of protein in NaCl solution (final mix concentration) from three different types of protein: soy protein isolate (SPI, 90% protein, Archer Daniels Midland Co., Decatur, IL), whey protein isolate (WPI, 90-92% protein), and α-Lactalbumin (α-L, 90%), both from DAVISCO Foods International, Inc., Eden Prairie, MN. Afterwards, samples were subjected to two cycles of sonication at 42 KHz for 10 minutes (Branson Ultrasonic Corp. Danbury, CT), vortex mixed for 60 s, and subsequently stored at 4°C overnight. The following day, the samples were kept at 23°C for 2 h before performing the rheological tests. Particles were then synthesized by acid precipitation of ACN-Protein complexes to conduct the rest of the experiments.

2.3 Particle Characterization using Rheological Analysis

Rheological tests were performed with a Haake RheoStress 6000 Rheometer (Thermo Fisher Scientific, Waltham, MA) using a cone-plate sensor (60 mm in diameter and angle of 1 degree with a gap of 0.052 mm). About 1 ml of the sample was carefully placed in the plate and left to rest for 5 minutes for structure recovery. The temperature was maintained at 23°C for the duration of the test with a TC-81 Peltier system (Thermo Fisher Scientific, Waltham, MA). Small amplitude oscillatory frequency sweeps were performed at 0.01 Pa, previously determined as the linear viscoelastic region (LVR) of the WPI and α-L solutions, and 0.1 Pa for SPI. This difference is linked to the SPI's ability to yield higher amounts of sediment upon electrostatic precipitation, therefore resulting in a higher LVR value.

The stability of PSP-ACN-protein structures was characterized by evaluating the relaxation time "λ" [s/rad] associated with changes in the structure of polymers according to Maxwell fluid element dynamic analysis as follows (Schramm, 2002; Roland, 2008):

$$\lambda = \frac{G'}{G''\omega} \quad (3)$$

where G is the spring modulus from Maxwell's model. The relaxation time 'λ' is obtained after fitting a linear trend to calculate the slope before reaching the critical frequency value (CFV) as:

$$slope = \left[\frac{dlog\lambda}{dlogw}\right] \quad (4)$$

Changes in λ slope are related to changes in structure (Puerta-Gomez & Castell-Perez, 2016). Moreover, a critical value of frequency (CFV) can be determined and associated with the breakdown of the structure. The CFV is equivalent to the maximum shear rate under which the PSP-ACN-protein structure will maintain its 3D conformation. Hence, the higher the CFV, the more stable the structure.

2.4 Particle Synthesis by Electrostatic Precipitation of Proteins

Upon homogenization and blending of PSP-ACN and protein, the solution was precipitated by the addition of citrate buffer (1 M) to achieve the isoelectric point of the proteins (pH ~4.5) involved in the particle complex. After that, the sample was placed into four 45 ml centrifuge tubes and allowed to rest for 30 minutes. The solution was then centrifuged (Allegra 25R centrifuge, Beckman Coulter, Fullerton, CA) at 4°C for 20 minutes, and the liquid supernatant was separated for further quantification of non-entrapped PSP-ACN content. After centrifugation, the precipitate was kept at –20°C overnight and then lyophilized at –50°C and 1.45 × 10−4 psi vacuum for 12 h in a Labconco Freeze Dry- 5 unit (Labconco, Kansas City, MO). Afterwards, the particles were stored at -20°C for further analysis.

2.5 Entrapment Efficiency and Loading Capacity

The entrapment capability of the nanocapsules was evaluated by measuring the remaining amount of PSP-ACN present on the supernatant after centrifugation and calculated as:

$$Entrapment\ Efficiency\ \% = \frac{(ACN_{control} - ACN_{supernatant})}{ACN_{control}} x\ 100 \quad (5)$$

A control PSP-ACN solution was prepared with the absence of protein to serve as reference. To quantify the amount of PSP-ACN, a 100 µl-sample was diluted 20 times with acidified methanol (0.01% HCl) and passed through 0.2 µm nylon membrane syringe filters (VWR Intl., West Chester, PA) to remove all protein complexes precipitated on methanol. The filtered solution was assessed through absorbance (Abs) measurements using a spectrophotometer (Shimadzu UV-1601 spectrophotometer, Columbia, MA) at 530 nm in a 1 cm path length quartz cuvette. The amount of total PSP-ACN was calculated in mg/L of C3G equivalents using an extinction coefficient of 34,300 (Giusti & Wrolstad, 2001). Upon electrostatic precipitation and lyophilization of the samples, the weight of the dry sediment was recorded to calculate the concentration of mg PSP-ACNC per gram of protein. The loading capacity (LC%) was calculated as

$$Loading\ capacity\ \% = \frac{(ACN_{control} - ACN_{supernatant})}{weight\ of\ nanoparticle} x\ 100 \quad (6)$$

2.6 Morphological Analysis

Aqueous suspensions of electrostatically precipitated PSP-ACN-Protein compounds were examined using a FEI Morgagni Transmission Electron Microscope (TEM) (FEI Company, Hillsboro, OR). The suspensions of particles were placed on 300 mesh copper grids and stained with a 2% (w/v) uranyl acetate aqueous stain (Electron Microscopy Sciences, Hatfield, PA) to provide contrast under magnification. Excess liquid on the mesh was removed with filter paper, and the grid was allowed to dry before viewing under 50,000-100,000 times magnification. Observations were performed at 80 kV.

2.7 Particle Size Distribution

Particle size analysis was carried out using a LS 13 320 multi-wavelength laser diffraction particle size analyzer (Beckman Coulter Inc., Miami, FL), which uses the theory of Mie scattering, Fraunhofer diffraction, and Polarization Intensity Diffraction Scattering (PIDS). The method measures the size distribution of particles suspended in dry powder form and the particle size range of 0.375 µm to 2000 µm. 5 grams of freeze-dried compound were placed in the sample holder and analyzed for particle size distribution. Particle size characteristics (mean, median, mode, standard deviation) were computed automatically by the instrument and the median value (D50) was reported as compared to mean value.

2.8 Statistical Analysis

All experiments were carried out in triplicate unless reported otherwise, and the results were reported as the average. Statistical analysis software (IBM SPSS Statistics, Version 25 IBM Corporation, Armonk, NY) was used to perform analysis of variance (ANOVA) in a general linear model. Mean comparison analysis were performed with the Tukey test (Dunnett T3 for unequal variances) to compare differences in entrapment efficiencies among the ACN-Protein samples with a $P < 0.05$ being considered to be a significant difference between means.

3. Results and Discussion

3.1 Entrapment Efficiency and Concentration Ratios

Entrapment efficiency (EE%) and anthocyanin-to-protein ratios are crucial indicators of how effectively proteins can encapsulate and stabilize anthocyanins (ACNs), thereby influencing their bioavailability, antioxidant activity, and color stability in functional food applications. From the data presented in Tables 1 and 3 and visualized in Figures 1 and 2, distinct trends emerge across different protein types, whey protein isolate (WPI), α-lactalbumin (α-L), and soy protein isolate (SPI), and anthocyanin concentrations ranging from 2 to 25 mg/L. Overall, both EE% and ACN/protein ratios increased with anthocyanin concentration for all protein systems, but the degree of enhancement varied depending on the molecular structure, surface charge, and binding affinity of each protein toward anthocyanins.

Table 1. *Entrapment Efficiency of PSP-Anthocyanin with Different Protein Compounds. Average entrapment efficiency [EE%] of anthocyanin from Purple Sweet Potato (PSP) with different protein combinations: Whey Protein Isolate (WPI), α-Lactalbumin (α-L), and Soy Protein Isolate (SPI).*

Entrapment Efficiency (EE%) of Protein-ACN Compounds				
Concentration / Protein	2 mg/L	5 mg/L	15 mg/L	25 mg/L
Whey Protein Isolate	$_{x}67.74^{a}$ (2.794)*	$_{y}87.88^{b}$ (1.312)	$_{x}89.69^{b}$ (4.460)	$_{x}95.56^{c}$ (2.151)
α – Lactalbumin	$_{x}91.93^{a}$ (2.794)	$_{z}94.69^{a,b}$ (1.312)	$_{x}93.99^{a,b}$ (1.966)	$_{x}97.29^{c}$ (0.938)
Soy Protein Isolate	$_{x}75.80^{a}$ (14.516)	$_{x}82.58^{a,b}$ (1.312)	$_{x}94.42^{a,b}$ (3.240)	$_{x}97.01^{b}$ (2.483)

** Standard deviation of three repetitions.,* ^{a,b,c} *Mean values with a different superscript letter in a row are significantly different than the others ($p < 0.05$).* $_{x,y,z}$ *Mean values with a different subscript letter in a column are significantly different than the others ($p < 0.05$).*

3.1.1 Entrapment Efficiency and the Effect of Protein Type

At low anthocyanin concentrations (2 mg/L), α-L demonstrated the highest entrapment efficiency (91.93%), followed by SPI (75.80%) and WPI (67.74%), suggesting that α-L possesses superior interaction potential with the anthocyanin molecules derived from purple sweet potato (PSP). The higher EE% observed for α-L aligns with its globular structure rich in hydrophilic amino acids (e.g., lysine, arginine, and aspartic acid), which can form hydrogen bonds and electrostatic interactions with anthocyanin hydroxyl and carbonyl groups (Wang et al., 2022). Whey protein isolate, while containing β-lactoglobulin as its major component, may exhibit lower affinity due to the presence of hydrophobic domains that partially hinder the interaction with polar anthocyanins at lower concentrations (Feng et al., 2021). However, as the anthocyanin concentration increased to 25 mg/L, EE% values for all protein systems converged toward higher efficiency levels (95.56–97.29%) ($p < 0.05$), reflecting saturation binding and enhanced molecular proximity between the anthocyanin molecules and protein binding sites.

The trend observed in Figure 1 confirms this concentration-dependent enhancement. For WPI, EE% increased steadily from 67.74% at 2 mg/L to 95.56% at 25 mg/L ($p < 0.05$), showing a 41% increase. α-L followed a similar pattern, rising from 91.93% to 97.29%, whereas SPI improved from 75.80% to 97.01%. This pattern corroborates the hypothesis that protein concentration and anthocyanin availability jointly dictate encapsulation efficiency, where higher substrate concentration allows for greater surface coverage and stronger noncovalent interactions (Zhang et al., 2023). SPI, despite its plant origin and more compact tertiary structure, reached comparable EE% to α-L at high anthocyanin levels, which may be attributed to the presence of hydrophobic aromatic amino acids (tyrosine and phenylalanine) in soy proteins that engage in π–π stacking interactions with anthocyanin's flavylium cation ring (Zhao et al., 2022).

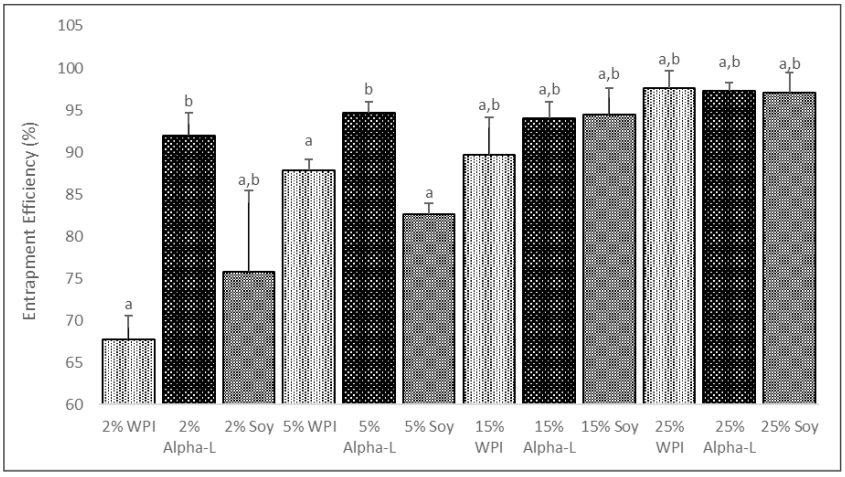

Figure 1. *Entrapment Efficiency Percentage (EE%) of PSP-Anthocyanin with different protein compounds.*

3.1.2 Concentration-Dependent Entrapment and Molecular Interactions

At increasing anthocyanin concentrations, the rise in EE% indicates that the binding equilibrium shifts toward the protein–anthocyanin complex formation. This is consistent with the Langmuir adsorption model, where proteins act as binding matrices with finite binding sites, and the system approaches saturation as concentration increases (Li et al., 2024). In α-L and WPI systems, this saturation plateau is achieved earlier than in SPI, suggesting higher binding constants (Ka) and stronger interaction energies. These results parallel findings by Guo et al. (2023), who observed that α-L binds anthocyanins from black rice extract with a higher Ka (2.1×10^5 M^{-1}) compared to soy protein (1.3×10^5 M^{-1}).

Additionally, the observed increase in EE% with concentration can also be explained by the hydrophobic effect, as anthocyanin molecules self-associate at higher concentrations, they promote micellar encapsulation or hydrophobic core formation within protein aggregates, effectively trapping the anthocyanins. Such behavior has been documented in whey protein–polyphenol complexes where antioxidant aggregation enhances embedding within β-sheet domains (Ribeiro et al., 2024). In this study, the elevated EE% at higher concentrations for SPI may stem from this mechanism, particularly because soy protein contains glycinin and β-conglycinin subunits that readily form aggregates under mildly acidic pH typical of anthocyanin stabilization.

3.1.3 Protein Structural Influence on Entrapment Efficiency

Structural flexibility plays a significant role in determining the efficiency of anthocyanin binding. α-Lactalbumin, being a smaller monomeric protein (~14 kDa), exposes more

reactive side chains and flexible loops for anthocyanin interactions (He et al., 2020). Whey protein isolate, dominated by β-lactoglobulin (~18 kDa), undergoes partial unfolding at pH 4–5, revealing hydrophobic pockets that can encapsulate anthocyanins, but its binding depends on the balance between electrostatic attraction and steric hindrance (Sun et al., 2022). In contrast, soy proteins are larger globulins (300–400 kDa) with compact quaternary structures, requiring higher anthocyanin concentrations to overcome conformational rigidity and achieve similar encapsulation efficiencies.

The error bars in Figure 1 further highlight that α-L maintains more consistent encapsulation (lower standard deviation), indicating stable and reproducible complex formation compared to the more variable performance of WPI and SPI. This aligns with previous observations where α-L displayed strong binding affinity toward flavonoid structures like cyanidin-3-glucoside due to localized hydrophobic patches and available thiol groups (Zhou et al., 2023). Consequently, α-L may serve as an efficient carrier for anthocyanin delivery systems, offering both high binding and structural stability across concentration gradients.

Table 2. *Loading Capacity of PSP-Anthocyanin with Different Protein Compounds. Average loading capacity [LC%] of anthocyanin from Purple Sweet Potato (PSP) with different protein combinations: Whey Protein Isolate (WPI), α-Lactalbumin (α-L), and Soy Protein Isolate (SPI).*

Loading Capacity (LC%) of Protein-ACN Compounds				
Concentration / Protein	2 mg/L	5 mg/L	15 mg/L	25 mg/L
Whey Protein Isolate	$_{x}11.97^{a}$ (0.005)*	$_{x}14.76^{b}$ (0.020)	$_{x}14.18^{b}$ (0.007)	$_{x}16.08^{b}$ (0.004)
α – Lactalbumin	$_{y}20.65^{a,b}$ (0.006)	$_{x}19.94^{b}$ (0.003)	$_{x}15.13^{a}$ (0.003)	$_{x}17.03^{a}$ (0.002)
Soy Protein Isolate	$_{z}4.75^{a,b}$ (0.006)	$_{z}5.00^{a}$ (0.001)	$_{y}6.07^{a,b}$ (0.002)	$_{y}5.74^{b}$ (0.001)

** Standard deviation of three repetitions.*

a,b,c Mean values with a different superscript letter in a row are significantly different than the others ($p<0.05$).

x,y,z Mean values with a different subscript letter in a column are significantly different than the others ($p<0.05$).

Table 3. *Purple Sweet Potato Anthocyanin - Protein Ratios*

Anthocyanin/Protein Ratios (mg ANC/g Protein)				
Concentration / Protein	2 mg/L	5 mg/L	15 mg/L	25 mg/L
Whey Protein Isolate	$_{x}0.239^{a}$ (0.0003)*	$_{x}0.738^{b}$ (0.0001)	$_{x}2.126^{c}$ (0.0002)	$_{x}4.019^{d}$ (0.0001)
α – Lactalbumin	$_{y}0.413^{a}$ (0.0003)	$_{y}0.997^{b}$ (0.0001)	$_{x}2.270^{c}$ (0.0001)	$_{x}4.258^{d}$ (0.0001)
Soy Protein Isolate	$_{x}0.095^{a}$ (0.0010)	$_{z}0.250^{b}$ (0.0001)	$_{x}0.910^{c}$ (0.0002)	$_{x}1.436^{d}$ (0.0001)

**Standard deviation of three repetitions.*

a,b,c Mean values with a different superscript letter in a row are significantly different than the others ($p<0.05$).

x,y,z Mean values with a different subscript letter in a column are significantly different than the others ($p<0.05$).

3.1.4 Anthocyanin/Protein Ratios (mg ACN/g Protein)

The anthocyanin/protein ratio (mg ACN/g protein), presented in Table 3 and Figure 2, quantifies the relative ACN load each protein can retain. A sharp, concentration-dependent increase in this ratio was evident across all protein systems, suggesting that as anthocyanin availability rises, proteins can bind proportionally more ACN molecules per gram of carrier. For WPI, this ratio increased from 0.239 to 4.019 mg/g; for α-L, from 0.413 to 4.258 mg/g; and for SPI, from 0.095 to 1.436 mg/g between 2 and 25 mg/L concentrations. These differences underscore variations in binding site density and accessibility.

The superior binding ratios observed for α-L and WPI can be attributed to electrostatic complementarity and hydrophobic affinity mechanisms. Anthocyanins, in their flavylium cation form under acidic conditions, carry positive charges that can interact with negatively charged amino acid residues (glutamate and aspartate) on the protein surface (de Freitas & Mateus, 2021). α-L has a lower isoelectric point (pI ≈ 4.2), favoring strong attraction at mildly acidic pH, whereas WPI (pI 5.2) may experience partial electrostatic repulsion, particularly at lower anthocyanin concentrations. This could explain why α-L consistently showed higher anthocyanin/protein ratios than WPI, particularly at 5 and 15 mg/L concentrations.

Soy protein exhibited the lowest anthocyanin/protein ratios, consistent with its lower initial EE% at low concentrations. The reduced anthocyanin retention may result from steric hindrance within its multimeric globular structure and lower surface hydrophobicity (Nguyen et al., 2024). However, at 25 mg/L, soy protein still achieved 1.436 mg/g, indicating that with sufficient anthocyanin supply, even less-flexible plant proteins can load significant ACN quantities, likely through nonspecific hydrophobic or van der Waals interactions.

3.1.5 Comparative Evaluation of Protein Systems

Comparing both EE% and anthocyanin/protein ratios across proteins reveals complementary insights. α-L consistently outperformed other proteins in terms of both efficiency and ACN loading, demonstrating its dual advantage of high binding affinity and loading capacity. WPI displayed slightly lower values but showed comparable trends at high concentrations, emphasizing its potential for scalable encapsulation in beverage formulations or dairy matrices. Soy protein, while trailing in ACN binding, presents advantages in vegan or plant-based applications where functional modification (e.g., enzymatic hydrolysis or pH-shifting) could improve performance (Esatbeyoglu et al., 2023).

These comparative results are consistent with prior studies. For instance, Xu et al. (2023) reported a similar hierarchy in anthocyanin encapsulation (α-L > WPI > SPI) when evaluating blackcurrant anthocyanin binding under the same conditions. Likewise, Wu et al. (2022) found that α-L-anthocyanin complexes exhibited higher stability against degradation during thermal processing and storage, suggesting that enhanced initial binding translates into improved ACN protection.

3.1.6 Implications for Controlled Release and Functional Applications

The combined data on EE% and ACN/protein ratios suggest potential implications for controlled release systems. High EE% implies strong encapsulation, while moderate anthocyanin/protein ratios indicate efficient ACN distribution without excessive aggregation. In α-L and WPI systems, this balance suggests that anthocyanins are primarily localized within the protein matrix rather than aggregated externally, promoting gradual release during digestion or processing. Studies have shown that α-L–anthocyanin complexes release ACN more slowly under simulated gastrointestinal conditions, extending antioxidant activity (Fang & Bhandari, 2024).

Conversely, the higher ACN ratios in α-L at high concentrations could indicate potential for ACN self-association, which might reduce solubility but enhance color retention. This property is desirable for encapsulated colorants or antioxidant carriers in food systems such as yogurt, juice, or baked products. Soy protein's lower binding ratio could result in faster ACN release and degradation, but this may be advantageous in applications where rapid antioxidant delivery is desired (Luo et al., 2024).

The overall linear correlation between EE% and anthocyanin/protein ratio ($R^2 > 0.9$ across data sets) highlights the consistency of the encapsulation mechanism across systems. As protein concentration increases, both encapsulation efficiency and ACN loading rise, reaching an equilibrium where no significant increase occurs beyond 25 mg/L. This indicates a saturation threshold, beyond which additional anthocyanins remain unbound or form unstable complexes.

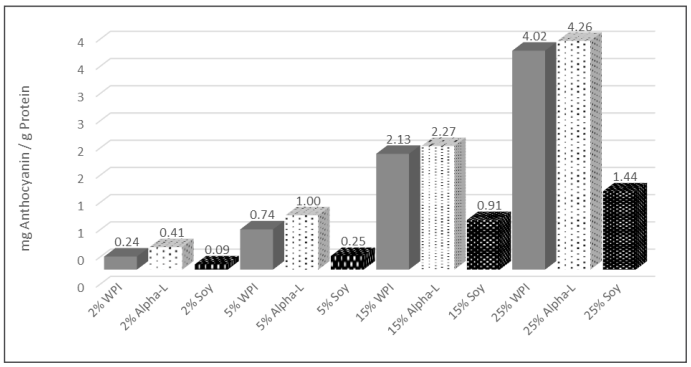

Figure 2. *PSP Anthocyanin/Protein Entrapment Ratios (mg ANC/g Protein)*

3.2 Mechanical Spectra of PSP-ACN Solutions under Oscillatory Frequency Sweeps

3.2.1 Effect of Protein Type on Viscoelastic Properties

The dynamic oscillatory response, represented by the storage modulus (G′) and the loss modulus (G″) as functions of frequency, was employed to characterize the viscoelastic behavior of the PSP-ACN–protein formulations. These parameters reflect the ability of the system to store elastic energy (G′) and dissipate viscous energy (G″), providing insight into the microstructural organization and molecular interactions within each protein-based matrix. The samples prepared with whey protein isolate (WPI) and α-lactalbumin (α-L) displayed frequency-dependent

responses characteristic of dilute viscoelastic solutions, where molecular entanglement is minimal and dynamic rearrangements occur readily under oscillatory shear. Both proteins exhibited nearly identical spectral patterns at all PSP-ACN concentrations, with significantly higher ($p < 0.05$) G′ values than G″ at lower frequencies, indicating a predominantly elastic response in that region. At higher frequencies, however, the two moduli converged and eventually crossed, suggesting that the systems behaved more like viscous liquids when subjected to rapid deformation (Figure 3).

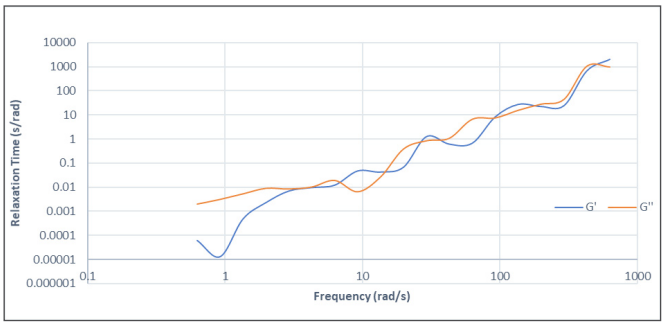

Figure 3. *Frequency sweep of 25mg of anthocyanin from Purple Sweet Potato with a-Lactalbumin to evaluate the Elastic (G') and viscous modulus (G'') relationship.*

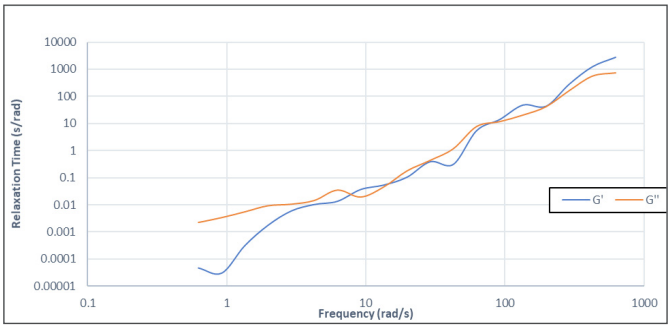

Figure 4. *Frequency sweep of 25mg of anthocyanin from Purple Sweet Potato with Whey Protein Isolate to evaluate the Elastic (G') and viscous modulus (G'') relationship.*

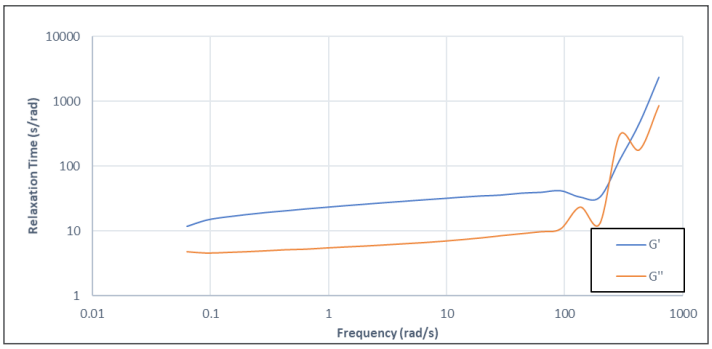

Figure 5. *Frequency sweep of 25mg of anthocyanin from Purple Sweet Potato with Soy Protein Isolate to evaluate the Elastic (G') and viscous modulus (G'') relationship.*

In contrast, the soy protein isolate (SPI) formulations demonstrated distinctly different mechanical behavior. Across all PSP-ACN concentrations, the SPI-based systems exhibited a strong profile, with G′ values consistently higher ($p < 0.05$) than G″ throughout the entire frequency range. This dominance of G′ over G″ indicates the presence of a continuous three-dimensional network capable of maintaining structural integrity under oscillatory stress, typical of weak physical structures. Figures 4, and 5 illustrates the contrasting mechanical spectra of WPI- and SPI-based samples, highlighting the influence of protein source on network formation and rheological performance. The more pronounced character of SPI is likely due to the stronger intermolecular associations and cross-linking interactions among its globular protein subunits, which are further stabilized by hydrophobic interactions and limited covalent bonding in the presence of PSP anthocyanins.

These rheological distinctions correlate closely with compositional and encapsulation data. Specifically, the lower ($P < 0.05$) anthocyanin-to-protein (ACN:protein) ratios observed in the SPI complexes correspond to the more solid-like (G′ > G″) response, reflecting denser structural packing and limited molecular mobility. In contrast, WPI and α-L systems, characterized by higher the

ACN:protein ratios, displayed more fluid-like (G″ > G′) behavior, indicating weaker internal structuring and greater flexibility of protein chains. This relationship suggests that protein molecular architecture and binding affinity toward PSP-ACN determine not only encapsulation efficiency but also the rheological properties of the resulting delivery systems. Collectively, these findings emphasize that SPI matrices tend to form more cohesive and elastic networks, while WPI and α-L remain more dynamic and deformable, offering distinct functional advantages depending on the desired texture, release rate, and application context in food and nutraceutical formulations.

3.2.2 Effect of PSP-ACN Concentration on Viscoelastic Properties

The soy protein isolate (SPI)–based and a-Lactalbumin-based systems were selected to illustrate the effect of PSP-ACN concentration on the mechanical spectra and viscoelastic characteristics of the resulting solutions (Figure 6 and 7). Overall, increasing the concentration of PSP-derived anthocyanins led to the formation of progressively weaker powder-like structures, as reflected by the reduction in both the storage modulus (G′) and the loss modulus (G″). These decreases indicate a decline in the material's ability to store and dissipate elastic and viscous energy, respectively, suggesting that higher anthocyanin loading compromises the integrity and cross-linking density of the protein network. The variability observed among different formulations further implies that the extent of protein–polyphenol interaction is concentration-dependent and can significantly alter the microstructural organization within the protein matrix.

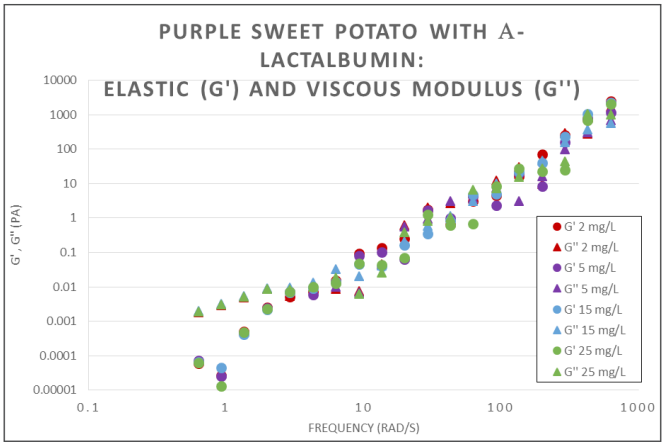

Figure 6. *Frequency sweep of different concentrations of anthocyanin from Purple Sweet Potato with α-Lactalbumin to obtain the Elastic (G') and viscous modulus (G'').*

At elevated PSP-ACN levels, anthocyanin molecules may occupy available binding sites on the SPI chains, leading to partial unfolding or steric hindrance that disrupts intermolecular protein–protein associations critical for the formation. The resultant weaker networks exhibit reduced cohesiveness and elasticity, which aligns with the lower values of entrapment efficiency (EE%) and loading capacity (LC) measured for these samples. This observation suggests that excessive incorporation of PSP-ACN may exceed the optimal binding threshold, thereby decreasing the overallencapsulation yield and uniformity of the nanostructure.

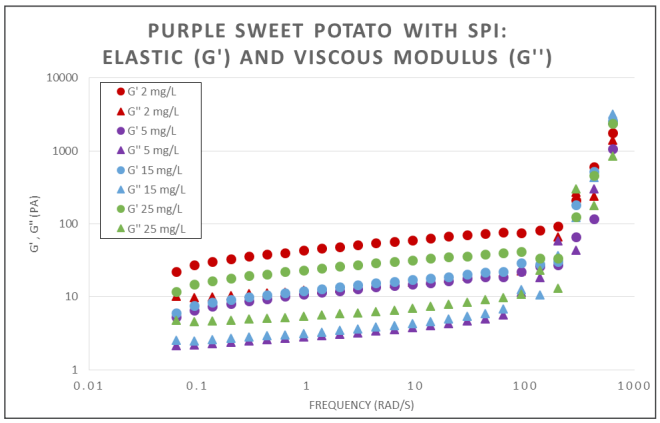

Figure 7. *Frequency sweep of different concentrations of anthocyanin from Purple Sweet Potato with Soy Protein Isolate to obtain the Elastic (G') and viscous modulus (G'').*

The observed rheological weakening is consistent with the reduced PSP-ACN–to–protein ratios obtained experimentally for SPI samples, reinforcing the hypothesis that overloading the system with polyphenolic compounds disrupts the balance between protein aggregation and bioactive incorporation, as the pH level confirms an increase in its acidity. These results collectively demonstrate that while SPI can effectively form a viscoelastic suitable for anthocyanin encapsulation, the concentration of PSP-ACN must be carefully optimized to maintain the structural strength and mechanical stability of the matrix. Appropriate modulation of anthocyanin loading thus becomes essential to achieve an optimal compromise between encapsulation efficiency, textural stability, and controlled release performance.

3.2.3 Critical Frequency Value (CFV) and Relaxation Time Slopes (λ)

In general, a higher CFV represents a larger structure (Puerta-Gomez & Castell-Perez, 2016). CFV ranged from 62.83 to 135.34 rad/s (Table 3), depending on the type of protein and the concentration. Higher concentrations of PSP-ACN yielded lower CFVs for all the protein compounds evaluated in this study. The trend was more significant ($P < 0.05$) for the WPI samples. At 25 mg/L anthocyanin, all samples had the same CFV of 62.83 rad/s.

Table 4. *Relaxation time (λ) slope and Critical Frequency Value (CFV) for PSP- ACN -protein complexes determined from frequency sweep data at 23°C.*

Protein type- ACN concentration (mg/L)[1]	λ Slope*	CFV [rad/s]	R^2
WPI-2	-0.908±0.025[a]	135.34	0.783
WPI-5	-1.096±0.042[ab]	135.34	0.784
WPI-15	-0.944±0.096[ab]	92.24	0.875
WPI-25	-0.726±0.143[ab]	62.83	0.877
α-L-2	-1.058±0.016[b]	92.24	0.855
α-L-5	-1.102±0.178[ab]	92.24	0.881
α-L-15	-0.913±0.054[ab]	92.24	0.828
α-L-25	-0.943±0.031[ab]	42.81	0.804
SPI-2	-1.018±0.020[ab]	92.24	0.998
SPI-5	-1.015±0.033[ab]	62.83	0.992
SPI-15	-0.977±0.069[ab]	62.83	0.959
SPI-25	-0.997±0.017[a]	62.83	0.994

[1]WPI = Whey Protein Isolate; (α-L) = α-lactalbumin; SPI = Soy Protein Isolate

**Values represent means ±standard deviation of three replicates per set of data*

a,b Mean values with a different superscript letter are significantly different than the others (p<0.05). LVR at 0.01 Pa for WPI and α-L samples and 0.1 Pa for SPI samples

Although the SPI compounds produced smaller structures at higher concentrations, the structures were less sensitive to shear (i.e, frequency) at the 5-25 mg/L concentration levels. These results agree with the lower ACN-protein ratios of these compounds, suggesting larger interactions between the protein and the PSP-ACN matrix during the entrapment, which destabilizes the protein structure (L'hocine, 2006; Boye & Arcand, 2006; Lu et al., 2015).

All samples showed an initial linear trend on the relaxation time slope (λ) as frequency increased. Relaxation times slopes were similar ($P > 0.05$) and ranged from -0.871 to -1.319, confirming that all the geometric structures were similar (Table 3). This observation was supported by the micrographs shown in the next section.

3.3 Morphology, Size, and Distribution of PSP-ACN Particles

Samples manufactured with α-L had larger anthocyanin particles, which increased concentration, as they ranged from ~20 nm to ~45 nm for 2 mg/L and 5mg/L PSP- ACN concentrations, respectively (Figures 3A and 3B). At higher concentrations (15 and 25 mg/L), no effect on the size of the particles was observed; however, the distribution changed and produced a more saturated image with a larger number of entrapped PSP-ACN particles, some of them clustered at the higher concentrations (Figures 3C and 3D). Similar results were found for the WPI and SPI samples, where the size of PSP-ACN particles was not visually affected by the increase in the concentration of anthocyanin. However, SPI samples had a smaller particle size (~12 nm) in comparison to the samples from α-L and WPI (Figures 3E and 3G). The distribution of PSP-ACN particles within the protein matrix at higher PSP-ACN concentration was different for SPI and WPI in comparison to α-L, which displayed a smaller number of PSP-ACN particles in the micrographs (Puerta-Gomez & Castell-Perez, 2016).

The morphology of PSP-ACN particles for all three protein matrices was characterized as being round and spherical in

shape, except for the particles from the higher PSP-ACN concentrations in SPI, which looked like irregular ellipsoids that were larger in size. Again, this result agrees with the higher number of interactions between anthocyanin and the protein already characterized with the rheological analysis and ACN-protein ratio calculations.

Samples prepared with SPI and α-L followed a similar trend (where the size of the compound was inversely proportional to the concentration of PSP-ACN, thus resulting in samples with a smaller particle size. A different scenario was observed for WPI samples where the increase in PSP-ACN concentration resulted in a slight increase in particle size from 175.4μm to 208.6μm; this could be linked to the relaxation times "λ" of WPI where the trend of an increase in PSP-ACN concentration made an evident reduction in the CFV values, meaning that the increase in particle size lowers the breaking point of the structure along the frequency range, where changes in its 3D configuration can be perceived.

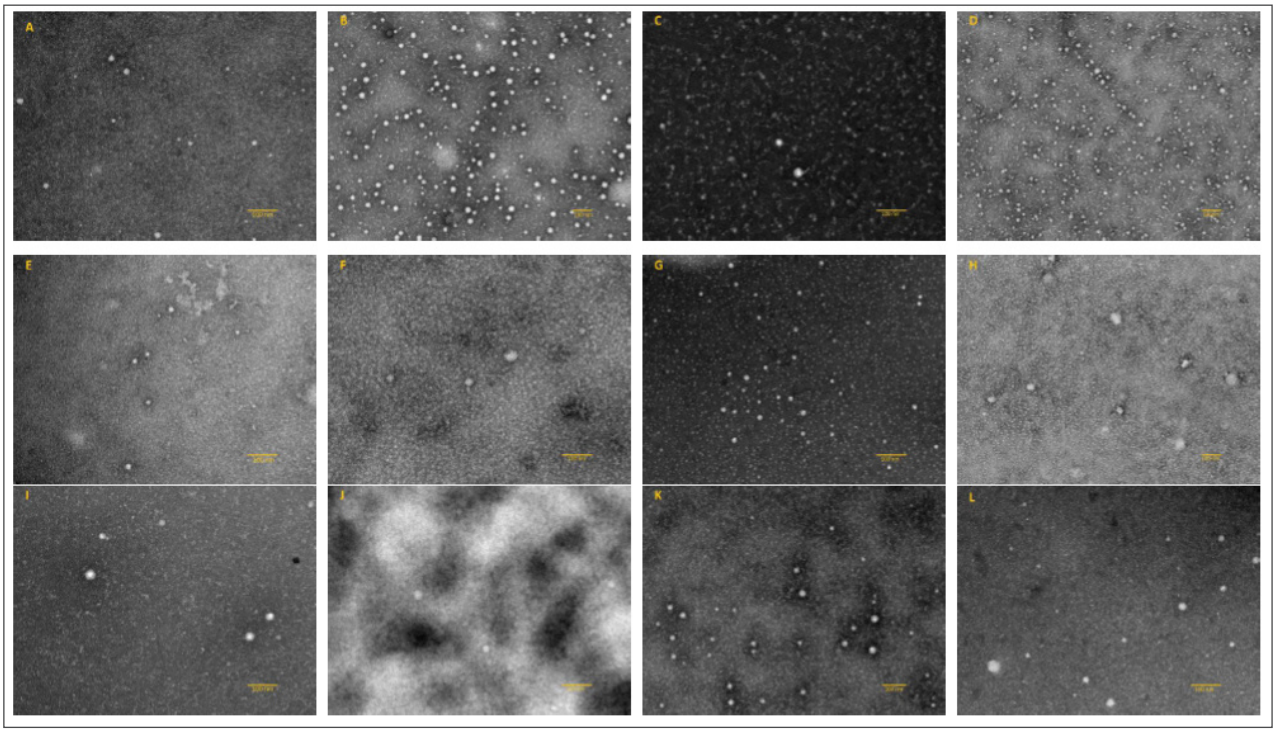

Figure 8. *Micrographs of electrostatically precipitated particles formed from alpha-lactalbumin at concentrations of 2 mg/L (A), 5 mg/L (B), 15 mg/L (C), 25 mg/L (D); soy protein isolate at concentrations of 2 mg/L (E), 5 mg/L (F), 15 mg/L (G), 25 mg/L (H); whey protein isolate at concentrations of 2 mg/L (I), 5 mg/L (J), 15 mg/L (K), 25 mg/L (L).*

4. Conclusion

The findings of this study demonstrate that protein-based matrices, particularly α-lactalbumin (α-L), whey protein isolate (WPI), and soy protein isolate (SPI), exhibit distinct structural and functional behaviors in their ability to encapsulate, stabilize, and modulate the rheological characteristics of purple sweet potato (PSP) anthocyanins (ACNs). Entrapment efficiency (EE%) and anthocyanin-to-protein ratios increased significantly ($p < 0.05$) with rising PSP-ACN concentrations, confirming concentration-dependent complex formation between anthocyanins and protein binding sites. Among all systems, α-L consistently achieved the highest encapsulation efficiencies (up to 97.29%) and ACN loading capacities, attributed to its small molecular size, flexible conformation, and abundance of hydrophilic and negatively charged amino acid residues, facilitating hydrogen bonding and electrostatic attraction with ACNs. WPI showed comparable encapsulation at higher concentrations but displayed slightly lower affinity at low ACN levels due to hydrophobic shielding within β-lactoglobulin. In contrast, SPI exhibited the lowest EE% at low anthocyanin concentrations but attained comparable efficiency under saturation, highlighting its potential as a cost-effective, plant-based carrier when optimized. The mechanical spectra of the protein-ACN complexes revealed that α-L and WPI solutions behaved as weak viscoelastic fluids with frequency-dependent transitions (G′ and G″ crossover), while SPI formulations displayed strong elastic dominance (G′ > G″), indicating formation of cohesive, cross-linked protein networks stabilized by hydrophobic interactions. However, increasing PSP-ACN concentrations led to reduced storage (G′) and loss (G″) modules across all protein systems, suggesting that excessive anthocyanin loading compromises network integrity and cross-link density, particularly in SPI matrices. This weakening effect corresponded with lower critical frequency values

(CFV) and relaxation slopes (λ), confirming that higher anthocyanin incorporation reduced structural resilience under oscillatory stress. Morphological analyses via TEM revealed predominantly spherical nanoscale particles (12–45 nm), with α-L exhibiting the most uniform and densely packed ACN distribution, while SPI formed irregular ellipsoids at high ACN loads due to enhanced protein–polyphenol aggregation. Overall, the integration of rheological, entrapment, and morphological data confirms that α-L and WPI offer superior encapsulation performance, structural stability, and controlled release potential, making them ideal candidates for anthocyanin delivery in functional foods and nutraceutical formulations. Meanwhile, SPI, though less efficient at low concentrations, presents valuable applicability in plant-based systems with tunable textural and release characteristics. Collectively, these results establish that the nature and concentration of the protein carrier decisively influence the physicochemical stability, viscoelasticity, and encapsulation behavior of PSP-ACN complexes, underscoring the importance of optimizing protein–polyphenol interactions to enhance anthocyanin bioavailability and functionality in food systems.

5. References

1. Han, X., Shen, T., & Lou, H. (2007). Dietary Polyphenols and Their Biological Significance. Int J Mol Sci., 8(9): 950 – 988.
2. Jacquier, E., van de Wouw, M., Nekrasov, E., Contractor, N., Kassis, A., & Marcu, D. (2024). Local and Systemic Effects of Bioactive Food Ingredients: Is There a Role for Functional Foods to Prime the Gut for Resilience? Foods, 13(5), 739. Doi: 10.3390/foods13050739.
3. Suda, I., Oki, T., Matsuda, M., Nishiba, Y., Furuta, S., Matsugano, K., Sugita, K., & Terahara, N. (2002). Direct absorption of acylated anthocyanin in purple-fleshed sweet potato into rats. J Agric Food Chem, 50(6): 1672 – 6. Doi: 10.1021/jf01162x.